Application of multilayer perceptron network and random forest models for modelling the adsorption of chlorobenzene on a modified bentonite by intercalation with hexadecyltrimethyl…

Article *in* Reaction Kinetics, Mechanisms and Catalysis · November 2021

DOI: 10.1007/s11144-021-02121-6

CITATIONS
4

READS
147

4 authors, including:

Salim Bousba
University of Constantine 3
15 PUBLICATIONS **156** CITATIONS
SEE PROFILE

Youghourta Belhocine
Université 20 août 1955-Skikda
45 PUBLICATIONS **406** CITATIONS
SEE PROFILE

Nabil Messikh
Université 20 août 1955-Skikda
13 PUBLICATIONS **167** CITATIONS
SEE PROFILE

Reaction Kinetics, Mechanisms and Catalysis
https://doi.org/10.1007/s11144-021-02121-6

Application of multilayer perceptron network and random forest models for modelling the adsorption of chlorobenzene on a modified bentonite by intercalation with hexadecyltrimethyl ammonium (HDTMA)

Nabil Bougdah[1,3] · Salim Bousba[2,4] · Youghourta Belhocine[1] · Nabil Messikh[1]

Received: 7 September 2021 / Accepted: 12 November 2021

Abstract
Prediction of adsorption capacity, one of the most important properties of any adsorbent-adsorbate system, is crucial for adsorption studies. In this investigation, two approaches such as multilayer perceptron (MLP) and random forest (RF) were used to predict the adsorption capacity of hexadecyltrimethyl ammonium modified bentonite to remove chlorobenzene (CB) from aqueous solution. The adsorption study was conducted in batch mode at different adsorption parameters. The results show that the adsorption processes were best described by Freundlich isotherm model, while the adsorption mechanism followed the pseudo-second order kinetics. It was observed that the structure of MLP model that give the best prediction consisted of three layers: input layer with four neurons, output layer with one neuron, and four neurons at hidden layer. The three important parameters for RF model were $n_{\text{tree}} = 500$, $m_{\text{try}} = 1$, and node size = 1. According to the results obtained, the MLP model provided slightly higher levels of accuracy with a consistently high coefficient of determination ($R^2 = 0.996$) and low root mean square error (RMSE = 0.00101) compared to RF model. ($R^2 = 0.969$, RMSE = 0.03008). Therefore, the initial concentration of CB with 35.29%, appeared to be the most influential parameter in the adsorption of CB on the modified bentonite.

Keywords Adsorption · Chlorobenzene · Multilayer perceptron network · Random forest · Relative importance variables

Symbols

A_T	Equilibrium binding constant
B	Heat of sorption

✉ Nabil Messikh
nabchem@yahoo.fr

Extended author information available on the last page of the article

Published online: 19 November 2021

C	Constant relevant to the thickness of the boundary layer
CB	Chlorobenzene
C_e	Equilibrium liquid phase concentration of CB [mmol/L]
C_0	Initial liquid phase concentrations of CB [mmol/L]
I_j	Relative importance of the jth input variable on the output variable
k_1	Pseudo first order rate constant
k_2	Pseudo second order rate constant
K_F	Freundlich constant [L/g]
K_L	Langmuir isotherm constant
k_p	Rate constant of the intra-particle diffusion model
m	Mass of the dry adsorbent [mg]
n	Freundlich exponent (dimensionless)
N_h	Number of hidden neurons
N_i	Number of input neurons
q_e	Adsorption capacity at equilibrium [mmol/g]
q_m	The maximum monolayer adsorption capacity [mmol/g]
q_t	Amount of CB adsorbed at time t
R	Universal gas constant [8.314 J/mol K]
T	Absolute temperature [K]
t	Time [min]
V	Volume of the solution [L]
W	Connection weights
x_{max}	Maximum value of variable
x_{min}	Minimum value of variable
x_{norm}	Normalized value of x_i
y_i	Neural network output
y_{i0}	Target output value
Superscripts 'i', 'h' and 'o'	Refer to input, hidden and output layers
Subscripts 'k', 'm'and 'n'	Refer to input, hidden and output neurons

Introduction

Chlorobenzene (CB) is an important raw material in dye, pharmaceutical, pesticide, paint, and other organic chemical industry, the discharged wastewater in this kind of enterprise often can be detected in high concentration chlorobenzene [1–3]. It has raised serious concerns because it is chemically stable, toxic, persistent, and bioaccumulative. The wide use of chlorobenzene in numerous industrial applications has led to its widespread release into the environment and consequent contamination of soil and water resources [4–7].

CB can accumulate in the human body through the food chain, causing many diseases such as cancer, teratogenesis, mutagenesis, anaesthetic effects, and can

damage the central nervous system [8, 9]. Because CB emissions have a strong negative impact on air quality and human health, increasing attention is being paid to its elimination. Several technologies have been developed to remove the CB from water such as biological treatment [8], pyrolysis [10], and various advanced oxidation processes (AOP) [11–15], adsorption process [16], and ion exchange [17]. However, the use of these methods is restricted due to the high cost [18]. Among the many methods available for the removal of CB from water, adsorption has been considered as one of the most economically promising techniques due to its ease to operate and most effectiveness [16, 18]. Adsorption mechanism is of complex nature and conventional mathematical modelling cannot be used to fully model and simulate adsorption data. This is because of the interaction of many adsorption process parameters, and thus, the resulting relationships are strongly nonlinear [19–22].

The application of multiple statistical approaches has recently received considerable attention in science and engineering. In recent years, several methods such as multiple linear regression (MLR) [23], artificial neural network (ANN) [21, 22], the adaptive neuro-fuzzy inference system (ANFIS) [24], response surface methodology [25], and random forest [26], are applicable for modelling the adsorption process. Among these approaches which demonstrated to have the ability to model and predict the systems with a high degree of complexity were Artificial Neural Network (ANN) and Random Forests (RF).

ANNs, inspired by biological nervous processing, are a parallel distribution processing method combined of neurons and weights and are based on the principle that highly connected system of simple processing elements. They can train complex interrelationships between inputs and outputs variables [27, 28]. Neurons are the basic element in ANN, which is linked to neurons in the next layer and there forming different types of ANNs. Weight values are gradually corrected during a training process to compare predicted outputs to known outputs by using the back-propagation process to minimize the errors [29].

On the other hand, the random forest (RF), developed by Breiman [30], is an approach for classification and regression that works by building a multitude of decision trees during learning. Unlike traditional classification and regression trees (CART), the RF method is characterized by its bootstrapping and randomized variable selection methods, which reduce the correlation between decision trees, also decreasing the variance of the model [16, 23]. When a random forest is used for function approximation or regression, it is called Random Forest Regression (RFR) or Regression Forests. In RF method, the structure where decision trees are formed is called forest. In the random forest, every decision is formed by selecting samples from the data set with the bootstrap technique and determining the number of random variables determined from all variables at every node [31]. The data not chosen to build the tree, defined as out of the bag (OOB) were used to estimate the prediction error [32]. The results of all such trees are subsequently combined and an estimate of target variables is obtained by averaging the individual trees' outputs.

This method has some advantages over other statistical modelling methods, such as the ability to model highly nonlinear dimensional relationships, resistance to overfitting, relative robustness concerning the presence of noise in the data, the

establishment of an impartial measure of the error rate, and the capacity to determine the relevance of the variable used [33, 34].

According to our knowledge, the comparison between the ANN and RF has not been applied to predict the adsorption capacity of CB on modified bentonite from aqueous solution. Therefore, in this study, our prime focus is on two algorithms, namely, artificial neural network (ANN) and random forest (RF). Recently, these algorithms have become quite popular in machine learning community due to their robustness, ability to generalize well on unseen data, ease of use and, implementation on real-world problems [35, 36]. The main aim of this work is to investigate the removal of CB from aqueous solution using HDTMA modified bentonite as an adsorbent. Four parameters, namely, contact time, adsorbent dose, initial concentration of adsorbate, and pH, were examined to see how they can affect the performance of the adsorption process. Artificial neural network (ANN) and random forest regression (RFR) models are used to predict the adsorption capacity of the adsorption process. The performance of both the ANN and RFR models were compared.

Materials and methods

The experiments were conducted using the natural bentonite from Hammam Boughrara (west Algeria) with the following chemical composition: SiO_2—69.4%, Al_2O_3—14.7%, Fe_2O_3—1.2%, MgO—1.1%, CaO—0.3%, Na_2O—0.5%, K_2O—0.8%, TiO_2—0.2%, As—0.05% and loss ignition—11% [37]. The cation exchange capacity (CEC) was found to be 97 meqg/100 g [38].

Preparation of HDTMA-bentonite

The sodium exchanged form of the bentonite (Na-bentonite) was prepared from Algerian natural bentonite according to the procedure described in our previous work [4]. To improve the adsorption capacity of natural bentonite, Na-bentonite has been modified with a cationic surfactant hexadecyltrimethylammonium bromide (HDTMA). The sodium-exchanged bentonite sample (20 g) previously modified using the ion exchange method was stirred magnetically for 48 h at room temperature with 200 mL of HDTMA aqueous solution [4, 39]. The prepared HDTMA-bentonite was washed with deionized water until a negative bromide test had been obtained with 0.1 M $AgNO_3$ (VWR Prolabo-chemical, Spain). It was dried in an oven at 65 °C for 24 h before use [40]. All physicochemical characteristics of the natural bentonite and the modified HDTMA-bentonite were well studied in our previous work [41].

Batch adsorption experiments

Chlorobenzene C_6H_5Cl (CB) was purchased from (Merck Schuchardt, Germany). The CB adsorption experiments were carried out by adding various amounts of HDTMA-bentonite (20–200 mg) to several CB concentrations (0.05–1 mmol/L) at

an initial pH between 2.5 and 12.02 at temperature 25 °C during different contact times (0–180 min). The solutions were then shaken at 300 rpm. A UV–visible spectrophotometer (Analytik Jena spectrophotometer) was used for the determination of CB concentration in the solution at 258 nm. The adsorption capacity of HDTMA-bentonite was calculated by:

$$q_e = \left(\frac{C_0 - C_e}{m}\right)V \tag{1}$$

Here C_0 and C_e are initial and equilibrium concentrations of CB (mmol/L), V is CB solution volume (L), m is the mass of HDTMA-bentonite (g).

Prediction models

In this study, both ANN and RF were employed to predict the adsorption capacity of CB on modified bentonite and to identify the main factors controlling the adsorption process.

Artificial neural network

ANN is one of the tools which have the capabilities to handle highly nonlinear systems. A great advantage of ANN models is that it is not necessary to know the mathematical relationships between input and output variables. Instead, they figure out these relationships through successive training [42]. Among different kinds of neural networks, multilayer perceptron (MLP) feed-forward neural network models are commonly applied in various fields of environmental engineering such as waste treatment [43], membrane process [44], adsorption [45], advanced oxidation [46].

Fig. 1 presents the proposed network structure. A large number of simple processing elements (neurons) are arranged in three layers: the input layer (independent variables), output layer (dependent variables), and one or more hidden layer(s) based on the complexity of the problem at hand. However, theoretical studies have shown that the single hidden layer is sufficient for an ANN to approximate any complex

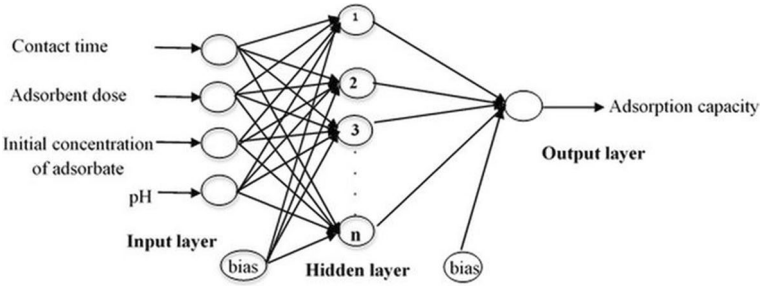

Fig. 1 Topology of the multilayer perceptron (MLP) network

nonlinear function [27, 47]. The general expression of MLP network can be given as:

$$y = f_2\left(\sum_{j=1}^{N} W_j f_1\left(\sum_{i=1}^{n} h_{ij}x_i + b_j\right) + b_0\right) \tag{2}$$

Here h_{ij}, b_j, and f_1 are the weight matrix, the bias vector and the activation function of the hidden layer, and w_j, b_o, and f_2 are the weight vector, the bias scalar, and the activation function of the output layer.

Neuron can employ any differentiable activation function to produce their output. According to the literature, it has been observed that the tangent sigmoid and hyperbolic tangent are the most used as activation functions in hidden layer [28, 44]. In this study, the tangent sigmoid transfer function (tansig) at hidden layer and a linear transfer function (purelin) at output layer were applied. Levenberg–Marquardt (LM) backpropagation was selected for training the designed networks.

The basic topology of the MLP network for predicting the removal of CB on the modified bentonite had four inputs corresponding to the batch adsorption process variables such as contact time (t), adsorbent dosage (m), initial concentration of CB (C_0), and pH. The output was the adsorption capacity (q_e). The total number of experimental data obtained from batch adsorption was 38. The data was devided into two categories, named the train and test data. Out of the whole number of data, about 80% of data equal to 28 was selected as the train set data, and about 20% of the data equal to 8 was selected as the test set data.

To ensure that each input variable provides an equal contribution in the MLP model, the inputs were scaled into a common numeric range of (− 1, 1) using Eq. 3.

$$x_{norm} = 2\frac{x - x_{min}}{x_{max} - x_{min}} - 1 \tag{3}$$

The model performance was evaluated using statistical parameters such as the coefficient of determination (R^2) and root mean square error calculated by the following Eqs. 4 and 5:

$$RMSE = \sqrt{\frac{1}{n}\sum\nolimits_{i=1}^{n}\left(y_{i0} - y_i\right)^2} \tag{4}$$

$$R^2 = 1 - \frac{\sum_{i=1}^{n}\left(y_{i0} - y_i\right)^2}{\sum_{i=1}^{n}\left(y_{i0} - \overline{y_i}\right)^2} \tag{5}$$

Random forest

Random forest (RF) is a classification and regression method, consisting of a combination of tree predictors where each tree is generated using a random vector sampled independently from the input vectors. When random forest method is

used for the resolution of function approximation or regression, it is called Random Forest Regression (RFR).

The RFR aims to decrease the correlation between the individual trees by bootstrapping (resampling with replacement) and randomized variable selection method, which results in diminished variance when the trees are aggregated as shown in Fig. 2. During the RFR model training, the main parameters that affect the estimation ability of random forest are the number of randomly selected variables used to grow each tree (m_{try}), the number of trees in the forest (n_{tree}), and the minimum number of terminal nodes for each tree (node size) [48, 49]. There are certain default values that have been suggested following empirical experiments on various data sets but one can use an optimizing tuning strategy with respect to prediction performance to select the most suitable values specifically for the data set under study [23].

In order to achieve the robustness and prediction accuracy model we have optimized the values of the parameters mentioned above using the trial-and-error method [50].

The formula for the predictions is given in Eq. 6 [22]:

$$y = \frac{1}{M}\sum_{i=1}^{M} T\left(x'\right) \tag{6}$$

Here y is the response, M is the number of trees after split and $T\left(x'\right)$ is a regression tree output.

The normalization applied to the experimental data for developing the RF model was identical to that used in the treatment of data when choosing the structure of MLP model, considering Eq. 3 and maintaining the same proportion of data used in training and testing steps 80% and 20%. The remaining 20% of data was used to test the model performance, which was assessed according to Eqs. 4 and 5.

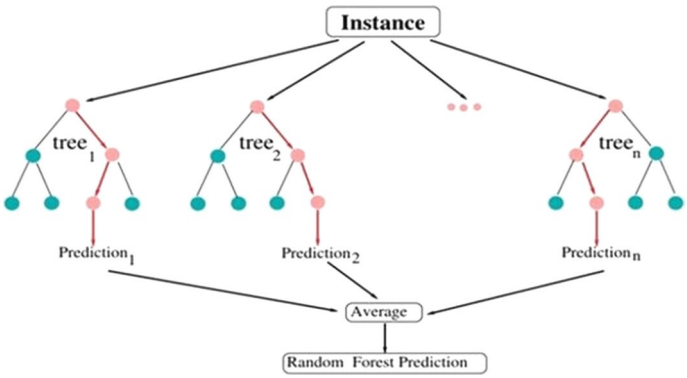

Fig. 2 Schematic diagram of RF model

Results and discussion

Adsorption isotherms

Equilibrium adsorption isotherms provide the most important information in understanding an adsorption process. Various isotherm models are available in the literature to test experimental isotherm values, from which Langmuir, Freundlich, and Temkin models were used to describe the relationship between the amount of CB adsorbed and its equilibrium concentration in solutions.

The Langmuir isotherm is based on the statement that adsorption takes place only at specific homogenous sites within the adsorbent surface with uniform distribution of energy level. Once the adsorbate attaches onto the adsorbent site, no further adsorption can take place at that site, and consequently the adsorption process is monolayer in nature. The non-linear form of the Langmuir equation is [41]:

$$q_e = q_m \frac{K_L C_e}{1 + K_L C_e} \tag{7}$$

Here q_m (mmol/g) is the theoretical maximum monolayer adsorption capacity, and K_L (L/mmol) is the Langmuir constant related to the energy of adsorption.

The fundamental characteristics of the isotherm of Langmuir can be expressed in terms of a dimensionless constant called the separation factor (R_L), defined by the following equation [51]:

$$R_L = \frac{1}{1 + K_L C_0} \tag{8}$$

The R_L value indicates whether the isotherm is either favorable ($0 < R_L < 1$), unfavorable ($R_L > 1$), linear ($R_L = 1$) or irreversible ($R_L = 0$) [52].

In Freundlich adsorption isotherm, the model assumes a heterogeneous surface with a non-uniform distribution of heat of adsorption over the surface. The Freundlich model is expressed as follows [52]:

$$q_e = K_F C_e^{1/n} \tag{9}$$

K_F, n are Freundlich constants, with K_F (L/g) indicating the sorption capacity and n (dimensionless) indicating the favorable nature of the adsorption process. In reality, the Freundlich constant (n^{-1}) explains the type of isotherm, when ($n^{-1} > 1$) the adsorption is unfavorable, ($n^{-1} = 1$) the adsorption is homogeneous and ($0 < n^{-1} < 1$) the adsorption is favorable [53].

The Temkin isotherm estimates that the decrease in the heat of adsorption is linear and the adsorption occurs through uniform distribution of binding energies rather than logarithmically, as implied in Freundlich isotherm. The Temkin isotherm is usually used for adsorption systems with heterogeneous surface energy (the distribution of adsorption heat is non-uniform). The non-linear form of the Temkin equation is represented as [54]:

$$q_e = B\ln(A_T C_e) \tag{10}$$

The regression coefficient of determination, R^2 was used as the basis for choosing the best appropriate isotherm for the adsorption process. The results are shown in Fig. 3 and Table 1.

The low R^2 value for the Temkin model suggests that this model was not suitable for describing the equilibrium adsorption data of CB on HDTMA-bentonite. The isotherm data was found to be more compatible with the Freundlich isotherm with R^2 of 0.966 with is higher than R^2 of the other adsorption isotherms (Table 1). The value R_L (0.916–0.355) indicates that the adsorption of CB on HDTMA-bentonite is favorable since $0 < R_L < 1$. Moreover, the intensity of adsorption, $\left(n^{-1}\right)$ was found to be 0.778. This value is less than one, it indicates that the adsorption of CB on HDTMA-bentonite is favorable [52]. Langmuir monolayer adsorption capacity was found to be 1.301 mmol/g.

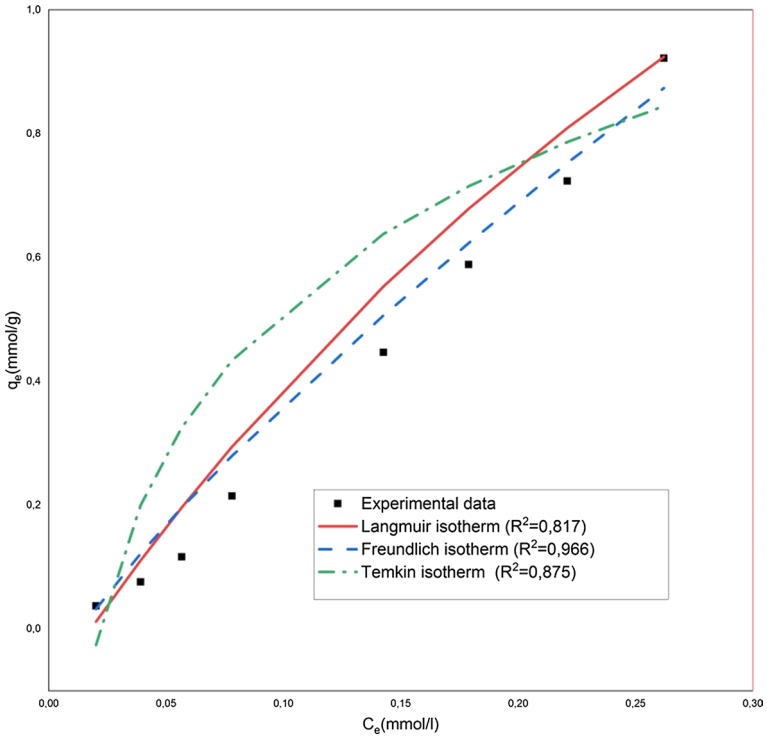

Fig. 3 Adsorption isotherms of CB on HDTMA-bentonite (m = 80 mg, C_0 = 0.01–1 mmol/L, t = 120 min T = 298 K, agitation speed = 300 rpm)

Table 1 Constants and determination coefficient of isotherms for adsorption of CB on HDTMA-bentonite

Isotherms	constants	Values
Langmuir	q_{max} (mmol/g)	1.301 ± 0.145
	k_L (L/mmol)	1.813 ± 0.157
	R_L	0.916–0.355
	R^2	0.817
Freundlich	K_F (L/g)	0.276 ± 0.018
	$1/n$	0.778 ± 0.021
	R^2	0.966
Temkin	A_T (L/mmol)	34.31 ± 2.631
	B	0.339 ± 0.027
	R^2	0.875

Adsorption kinetics

The kinetics of adsorption of CB using modified bentonite has been evaluated. The experimental data were examined by pseudo-first order kinetics, pseudo-second-order kinetics and intraparticle diffusion to understand the dynamics of adsorption process.

The non-linear form of the pseudo-first order model [55], also known as the Lagergren kinetic equation, describes the quantity of adsorbate on the heterogeneous adsorbent surface over time, according to Eq. 11:

$$q_t = \left(q_e - e^{-k_1 t}\right) \tag{11}$$

The non-linear form of the pseudo second order model is founded on the supposition that the rate limiting step may be chemisorption which involves electron exchange between the adsorbate and the adsorbent or valence forces by sharing [55]. Its expressed by Eq. 12:

$$q_t = \frac{k_2 q_e^2 t}{\left(1 + k_2 q_e t\right)} \tag{12}$$

The intra-particle diffusion model is plotted by q_t vs. $t^{0.5}$. If a straight line is obtained and passes through the origin, it indicates that the adsorption is controlled by intra-particle diffusion, otherwise, the intra-particle diffusion process is not the only step to control the adsorption process [33]. The equation is expressed as:

$$q_t = k_p t^{0.5} + C \tag{13}$$

All the constants of these models were estimated by non-linear and linear regression, and the results are listed in Table 2 and Fig. 4. The pseudo second order kinetic model fits well with the adsorption process with a good correlation value. Further, the calculated value of equilibrium adsorption capacity using the pseudo second order equation is close to the experimentally determined value (0.2143 mmol/g).

Table 2 Kinetic parameters for CB adsorption on HDTMA-bentonite

Pseudo-first-order			Pseudo-second-order			Intra-particle diffusion		
k_1 (min^{-1})	$q_{e\ calculated}$ (mmol/g)	R^2	k_2 (g/mmol/min)	$q_{e\ calculated}$ (mmol/g)	R^2	K_{int}	C	R^2
0.1748 ± 0.0216	0.1978 ± 0.0083	0.5947	0.3313 ± 0.0348	0.2327 ± 0.0039	0.9785	0.0119 ± 0.0012	0.0909 ± 0.0098	0.9567

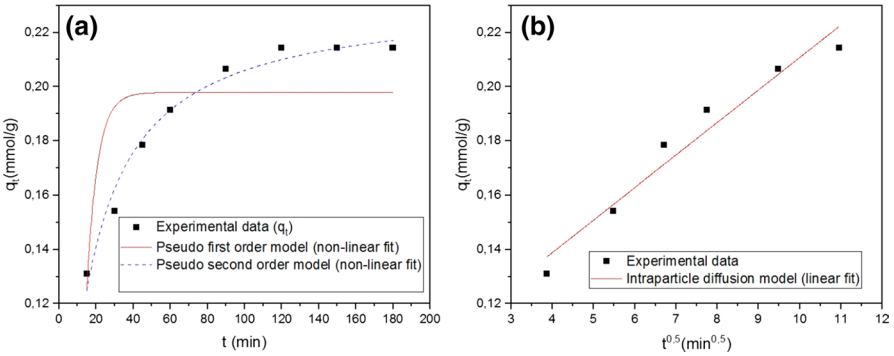

Fig. 4 Adsorption kinetics of CB: **a** pseudo-first order and pseudo second order, **b** intra-particle diffusion model (m = 80 mg, C_0 = 0.25 mmol/L, T = 298 K, agitation speed = 300 rpm, t = 15–180 min)

The mass transfer of adsorbate to the adsorbent is responsible for more than one factor, such as pore diffusion, film diffusion, and surface diffusion [54, 56]. The influence of such factors is well explained by the intra-particle diffusion model. As shown in Fig. 4b, the plots present a linear relationship but did not pass through the origin, suggesting that the intraparticle diffusion was not the only rate-controlling step and other rate-limiting steps may be involved and affect the adsorption of CB.

Model prediction

The purpose of this work was to test the ability of MLP and RF to model the non-linear relationship between the inputs and output variables. First, the parameters of both MLP and RF models must be optimized to perform the complicated non-linear mapping between the adsorption capacity and the batch adsorption process variables.

For MLP model, the important steps in developing MLP models are to determine the number of neurons at hidden layer. The performance of MLP networks was examined by varying the number of neurons arranged in the hidden layer from one to ten. The best structure of MLP model was chosen based on the minimum value of RMSE. An MLP with four neurons at hidden layer had the lowest value of RMSE (0.00101) as shown in Fig. 5. Moreover, when the number of neurons in the hidden layer exceeds 5, the RMSE remains constant. Therefore, the value of 4 for hidden neurons is selected as an optimum case.

Fig. 6 illustrates the comparison between experimental data and predicted values of adsorption capacity of CB on the modified bentonite using an MLP model, in the training and testing steps. The MLP model results shown a high coefficient of determination, not only at the training stage ($R^2 = 0.996$) but also at the testing stage ($R^2 = 0.962$), which implies that the MLP model fits well the experimental values of adsorption capacity.

From the above description of the RF model, it is evident that there are three parameters whose values need to be fixed prior namely: n_{tree}, m_{try}, and size node. The range turning parameters and the coefficient of determination R^2 obtained as

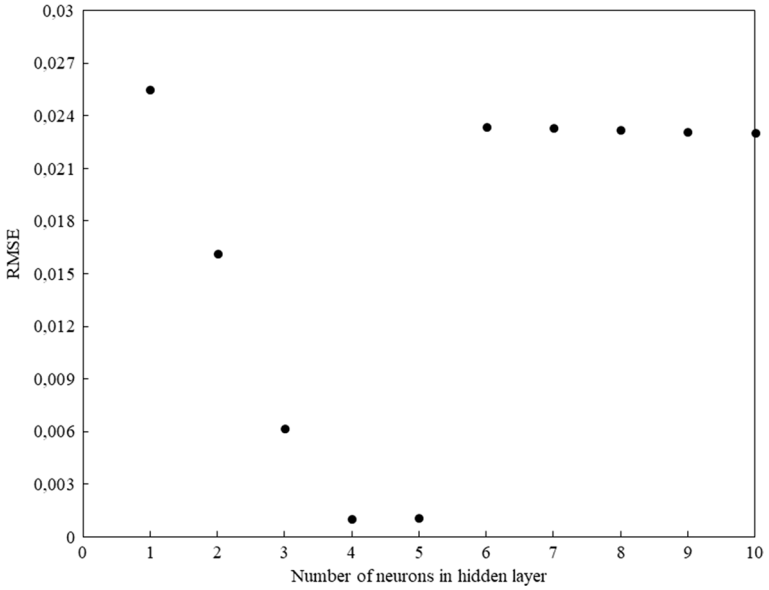

Fig. 5 Variation of RMSE vs number of neurons in hidden layer (Levenberg–Marquardt backpropagation, tansig transfer function at hidden layer, purelin transfer function at output layer

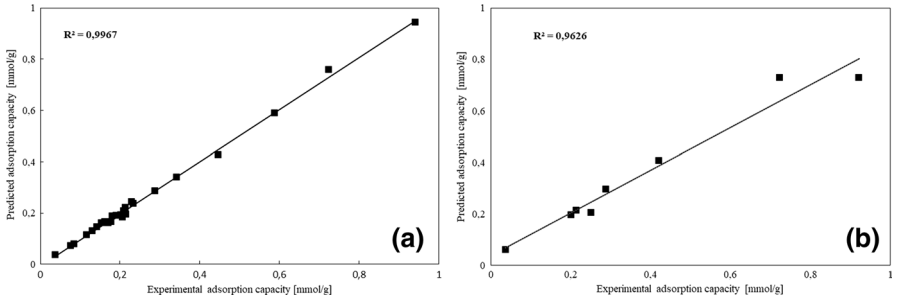

Fig. 6 Comparison between the experimental data and predicted values of adsorption capacity of CB on the modified bentonite using MLP model **a** training stage, **b** testing stage (LM backpropagation, tansig and purelin transfer functions at hidden and output layer, four neurons at hidden layer)

well as RMSE for training were summarized in Table 3. The results include only the values of R^2 above 0.90. It can be seen that the increase in the number of trees (n_{tree}) between 100 and 1500, there was no significant difference between the lower and higher values of R^2 and RMSE.

This might be due to the fact that when the number of trees in the forest is increased above the optimum, there is a general increase in computational expense, but the results do not improve significantly [57]. Generally, a large number of trees allows each variable to have a positive impact on the accuracy of random forest forecasts and that each variable has a sufficient chance of being included in the forest forecasting process [58].

Table 3 Evaluation of tuning parameters of RF model

n_{trees}	m_{try}	Node size	R^2	RMSE
100	1	1	0.9689	0.03607
	4	1	0.9688	0.03614
200	1	1	0.9771	0.03100
	2	1	0.9770	0.03104
	4	1	0.9770	0.03105
300	2	1	0.9750	0.03222
	4	1	0.9750	0.03233
500	1	1	0.9784	0.03008
	2	1	0.9784	0.03010
	4	1	0.9783	0.03011
1000	1	1	0.9772	0.03091
	2	1	0.9772	0.03093
1500	1	1	0.9771	0.03094
	2	1	0.9771	0.03095
	4	1	0.9771	0.03096

As shown in Table 3 the smallest RMSE and the highest R^2 values were 0.03008 and 0.9784. According to results obtained, the parameters were selected with values of $n_{tree} = 500$, $m_{try} = 1$, and node size = 1.

The comparison between the RF model results and the experimental data for both training and testing stages are depicted in Fig. 7. It was observed that in both stages the coefficient of determination is 0.969 and 0.94. These results confirm that the RF model succeeded in the prediction of the adsorption capacity of CB using the modified bentonite.

Both MLP and RF models were very accurate with high R^2 values, all above 96%. However, the MLP model showed slightly better than RF based on the determination coefficient and root mean square error values. Similar results were obtained for the adsorption of the methyl violet and Rhodamine 6G on magnetic walnut shell, and

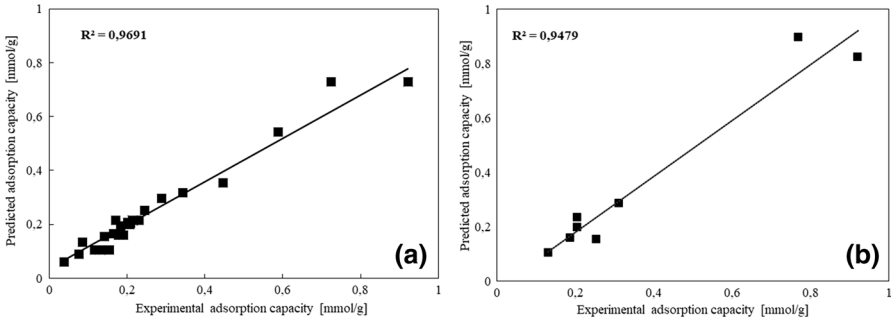

Fig. 7 Comparison between the experimental data and predicted values of adsorption capacity of CB on the modified bentonite using RF model **a** training stage, **b** testing stage ($n_{tree} = 500$, $m_{try} = 1$, and node size = 1)

adsorption of safranin-O and methyl violet dyes onto modified pince cone powder [59, 60]

Effect of contact time

The effect of the contact time on the adsorption capacity of CB using the modified bentonite can be seen in Fig. 8. It has been observed that the adsorption capacity of CB increases with increasing time and reaches a maximum value at the equilibrium time (120 min), and thereafter it remains constant. So, 120 min was selected as the optimal contact time for subsequent experiments. In addition, the optimized MLP and RF models were applied to predict the effect of contact time on CB removal by the modified bentonite. Fig. 8 clearly portrays that the predicted adsorption capacity values were in strong coherence with those of experimental data. This justified that both models were able to predict the influence of contact time with a high degree of coherency. For MLP model it is clear that the estimation of adsorption capacity of CB is more satisfactory than RF model.

Effect of the adsorbent dose

The influence of adsorbent dose on adsorption capacity of CB (0.25 mmol/L) was studied in the range of 20–200 mg and shown in Fig. 9. From this figure, it was observed that the adsorption capacity was higher when its adsorbent dose was lower. An increase of adsorbent dose above 60 mg does not change the CB removal percentage (68.8%). This may be explained by the saturation point

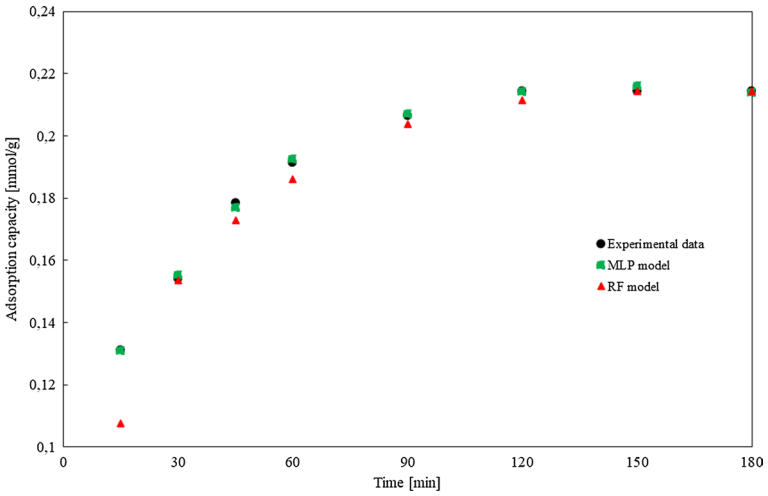

Fig. 8 Effect of contact time on CB removal by the modified bentonite (black markers: m = 80 mg C_0 = 0.25 mmol/L, t = 120 min, pH 6.75, agitation speed = 300 rpm, green markers: LM backpropagation, tansig and purelin transfer functions at hidden and output layer, 4 neurons at hidden layer, red markers: n_{tree} = 500, m_{try} = 1, and node size = 1). (Color figure online)

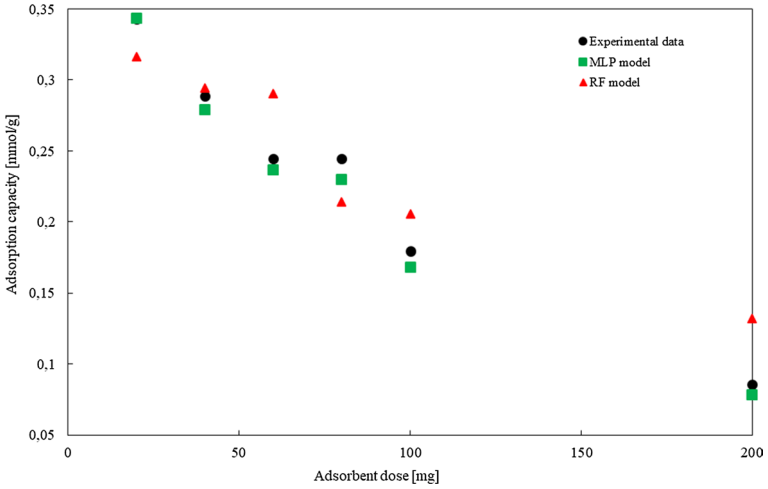

Fig. 9 Effect of adsorbent dose on CB removal by the modified bentonite (black markers: $C_0 = 0.25$ mmol/L, t = 120 min, pH = 6.75, agitation speed = 300 rpm, green markers: LM backpropagation, tansig and purelin transfer functions at hidden and output layery, four neurons at hidden layer, red markers: $n_{tree} = 500$, $m_{try} = 1$, and node size = 1). (Color figure online)

reached when the adsorbent dosage is increased; hence no further CB adsorption takes place. These results visibly indicate that the adsorbent dose must be fixed at 80 mg which is the adsorbent dose that corresponds to the minimum amount of adsorbent that leads to constant CB removal percentage. The estimated adsorption capacity of CB obtained with MLP model and RF model are given also in Fig. 9. According to this data, it can be observed that the predictions of both models have a good agreement with the experimental data. The curves generated by both MLP and RF models are "noisy", but are much closer to the experimental data. This behavior is probably due to nosier dataset. The accuracy of MLP model is higher than the second model used.

Effect of initial adsorbate concentration

Fig. 10 shows the influence of initial CB concentration on adsorption capacity in the range of 0.05–1 mmol/g. This comportment may be attributed to the fact that increasing concentration provides an increasing driving force to overcome all mass transfer resistances of the CB molecules between the aqueous and solid phases, leading to an increased equilibrium uptake capacity until adsorbent saturation is achieved [61].

The predicted data generated by both MLP and RF models faithfully followed experimental data in the range of initial CB concentration. The simulation results indicated that MLP approach provides more accurate prediction in comparison with RF approach.

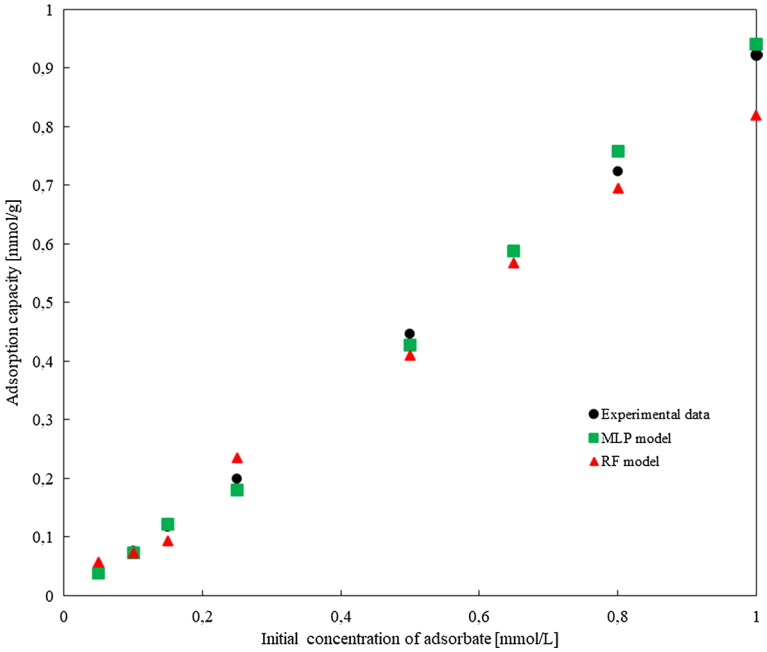

Fig. 10 Effect of initial concentration on CB removal by the modified bentonite bentonite (black markers: m = 80 mg, t = 120 min, pH 6.75, agitation speed = 300 rpm, green markers: LM backpropagation, tansig and purelin transfer functions at hidden and output layer, four neurons at hidden layer, red markers: $n_{tree} = 500$, $m_{try} = 1$, and node size = 1). (Color figure online)

Effect of pH

The pH of solution is one of the most crucial parameters for the adsorption process which can affect the surface proprieties of the adsorbent [62]. The experiments were carried out at various pH from 2.5 to 12.02. The effect of pH on the adsorption capacity of CB is illustrated in Fig. 11. It can be noted that the amounts uptake was increased from 2.5 to 8.14 and reached the maximum adsorption capacity of 0.2310 mmol/g at pH 8.14 and then declined after pH 8.14. This may be due to a very high dependence between the adsorption process and pH [40, 62]. Meanwhile, Fig. 11 shows the comparison between the predicted adsorption capacity generated by MLP and RF models at different pH. It was found that the two models give a satisfactory performance on the prediction of the experimental data when pH is below 6.8. The RF model was able to predict the adsorption capacity of CB with reasonable accuracy with slightly underestimation values at pH 8.14 and 10.09.

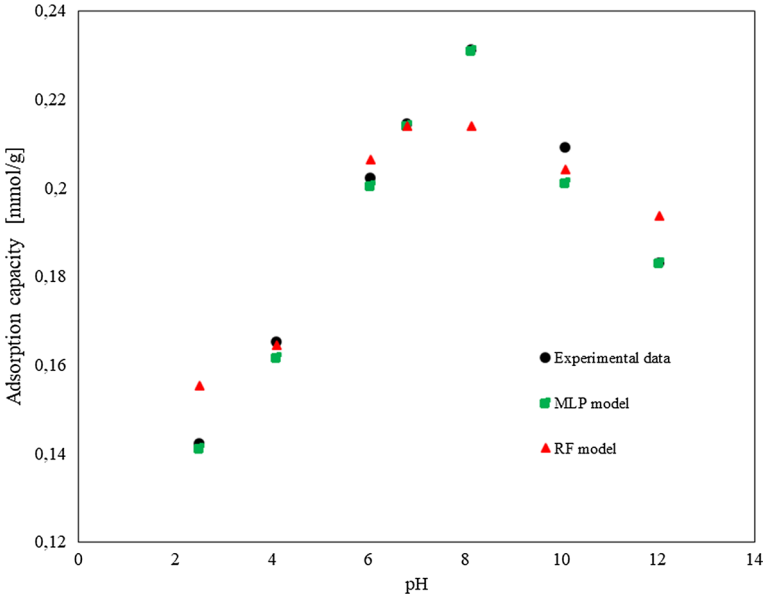

Fig. 11 Effect of pH on CB removal by the modified bentonite (black markers: m = 80 mg, C_0 = 0.25 mmol/L, t = 120 min, agitation speed = 300 rpm, green markers: LM backpropagation, tan-sig and purelin transfer functions at hidden and output layer, four neurons at hidden layer, red markers: n_{tree} = 500, m_{try} = 1, and node size = 1). (Color figure online)

Relative importance in inputs variables

The relative importance of different input variables on the adsorption capacity was determined based on the MLP model which is a slightly better approach than the RF model in this work. The level of each input variables corresponding to predict output variable can be obtained through the neural weight matrix listed

Table 4 Matrix weights: W_1:weights between input and hidden layers, W_2: weights between hidden and output layers

Neurons	W_1					Neurons	W_2
	Variables				Bias		Weights
	Time	Adsorbent dose	Adsorbate concentration	pH			
1	1.5716	2.1113	− 2.2640	− 0.5405	0.2296	1	0.9888
2	− 0.0760	1.1622	− 1.8995	− 1.8605	0.7576	2	1.6392
3	1.1583	− 2.0112	2.5512	0.3556	1.8471	3	2.7202
4	0.4991	− 1.1680	− 1.1095	− 0.8956	0.3905	4	4.3917
						Bias	− 0.2453

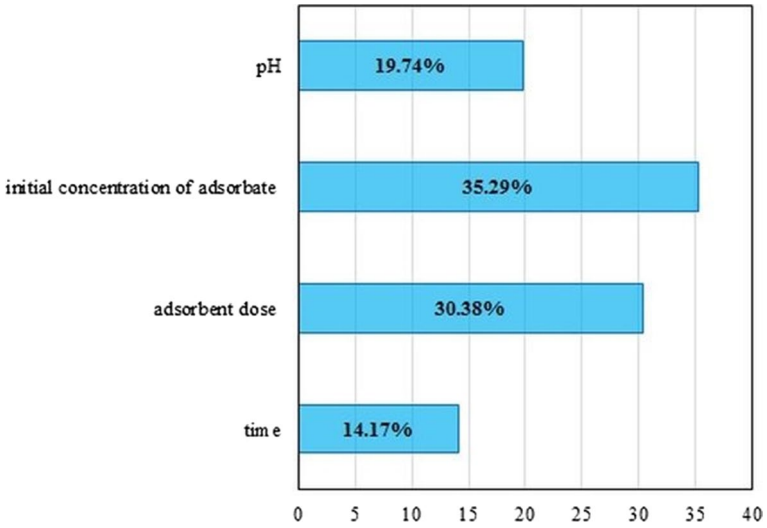

Fig. 12 Relative importance (%) of the input variables on the value of adsorption capacity of CB (the results were obtained from Eq. 13 using the neural weight matrix listed in Table 4)

in Table 4. Garson proposed an equation based on partitioning of connection weights [63]:

$$I_j = \frac{\sum_{m=1}^{m=N_h}\left[\left(\frac{\left|W_{jm}^{ih}\right|}{\sum_{k=1}^{N_i}\left|W_{km}^{ih}\right|}\right)\left|W_{mn}^{ho}\right|\right]}{\sum_{k=1}^{k=N_i}\left\{\sum_{m=1}^{m=N_h}\left[\left(\frac{\left|W_{km}^{ih}\right|}{\sum_{k=1}^{N_i}\left|W_{km}^{ih}\right|}\right)\left|W_{mn}^{ho}\right|\right]\right\}} \tag{14}$$

The relative importance variables calculated by Eq. 14 are depicted in Fig. 12. As can be seen, all the values of relative importance for parameters were above 10%, indicating that all of variables had strong effects on the adsorption capacity. The initial concentration of CB and the dose of adsorbent with relative importance of 35.29% and 30.80% appeared to be more influential parameters in the adsorption capacity of CB on the modified bentonite, followed by pH and time with the relative importance of 19.74% and 14.17%. Several studies have reached similar conclusions but with a differentiation in the order of the importance of the variables [64–66]. It seems that the most influential variable depended upon the experimental ranges adopted in the fitting model.

Conclusion

In this study we presented an application of two modelling techniques, that is, the MLP and RF, to model the adsorption process for predicting the adsorption capacity of CB using HDTMA-bentonite as an adsorbent. We first conduct the

adsorption study of CB onto HDTMA-bentonite in batch mode at different operating parameters. To construct our forecast models, we split the collected adsorption data into a training set and a test set. Based on the results of our investigation, we conclude that both multilayer perceptron network and random forest can be used successfully to predict the adsorption capacity of chlorobenzene onto HDTMA-bentonite. Also, the comparison of the results of the MLP model with four neurons at the hidden layer and RF model indicates that the MLP model predicted the adsorption capacity of CB with more accuracy than the RF model in terms of R^2 and RMSE. The relative importance investigation showed that all of the studied parameters (contact time, adsorbent dose, initial concentration of CB, and pH) have a significant influence on the adsorption process; however, the effect of initial concentration of CB with a relative importance of 35.29% is the most influential on the adsorption capacity of CB using HDTMA-bentonite.

References

1. Wijk DV, Thompson RS, Rooij CD, Garny V, Lecloux A, Kanne R (2004) Monochlorobenzene marine risk assessment with special reference to the Osparcom region: North Sea. Environ Monit Assess 97:69–86. https://doi.org/10.1023/B:EMAS.0000033042.01768.3f
2. Zhao X, Zang X, Qin Y, Li X, Zhu T, Tang X (2018) An experimental and theoretical study of the adsorption removal of toluene and chlorobenzene on coconut shell derived carbon. Chemosphere 206:285–292. https://doi.org/10.1016/j.chemosphere.2018.04.126
3. Zhu R, Mao Y, Jiang L, Chen J (2015) Performance of chlorobenzene removal in a nonthermal plasma catalysis reactor and evaluation of its byproducts. Chem Eng J 279:463–471. https://doi.org/10.1016/j.cej.2015.05.043
4. Bougdah N, Messikh N, Bousba S, Djazi F, Magri P (2020) Removal of chlorobenzene by adsorption from aqueous solution on the HDTMA-bentonite as a function of HDTMA/CEC ratio. Curr Res Green Sustain Chem 3:100038. https://doi.org/10.1016/j.crgsc.2020.100038
5. Cepeda EA, Iriate U, Sierra I (2014) Kinetic and thermodynamic study of chlorobenzene adsorption from aqueous solution onto granular activated carbon. Lat Am Appl Res 44:141–147
6. Gole VL, Gogate PR (2013) Intensification of sonochemical degradation of chlorobenzene using additives. Desalin Water Treat 53:2623–2635. https://doi.org/10.1080/19443994.2013.862743
7. Jose J, Philip L (2019) Degradation of chlorobenzene in aqueous solution by pulsed power plasma: mechanism and effect of operational parameters. J Environ Chem Eng 6:103476. https://doi.org/10.1016/j.jece.2019.103476
8. Cheng Z, Li C, Kennes C, Ye J, Chen D, Zhang S, Chen J, Yu J (2017) Improved biodegradation potential of chlorobenzene by mixed fungal-bacterial consortium. Int Biodeterior Biodegradation 123:276–285. https://doi.org/10.1016/j.ibiod.2017.07.008
9. Ramu AG, Muthuraman G, Moon IS (2020) Consistent room temperature electrochemical reduction of gaseous chlorobenzene to value-added intermediates by electro scrubbing. J Ind Eng Chem 89:334–338. https://doi.org/10.1016/j.jiec.2020.05.028
10. Vin N, Leclerc FB, Le Gall H, Sebbar N, Bockhorn H, Trimis D, Herbinet O (2018) A study of chlorobenzene pyrolysis. Proc Combust Inst 37:399–407. https://doi.org/10.1016/j.proci.2018.05.067
11. Dewulf J, Langenhove HV, Visscher AD, Sabbe S (2001) Ultrasonic degradation of trichloroethylene and chlorobenzene at micromolar concentrations: kinetics and modelling. Ultrason sonochem 8:143–150. https://doi.org/10.1016/S1350-4177(00)00031-6
12. Lee CL, Jou CJG, Huang H (2009) Degradation of chlorobenzene in water using nanoscale Cu coupled with microwave irradiation. J Environ Eng 136:412–416. https://doi.org/10.1061/(ASCE)EE.1943-7870.0000163

13. Liu L, Zhao G, Wu M, Lei Y, Geng R (2009) Electrochemical degradation of chlorobenzene on boron-doped diamond and platinum electrodes. J Hazard Mater 168:179–186. https://doi.org/10.1016/j.jhazmat.2009.02.004
14. Liua X, Chena L, Zhua T, Ning R (2019) Catalytic oxidation of chlorobenzene over noble metals (Pd, Pt, Ru, Rh) and the distributions of polychlorinated by-products. J Hazard Mater 363:90–98. https://doi.org/10.1016/j.jhazmat.2018.09.074
15. Sedlak DL, Andren AW (1991) Oxidation of chlorobenzene with Fenton's reagent. Environ Sci Technol 25:777–782. https://doi.org/10.1021/es00016a024
16. Sennour R, Mimane G, Benghalem A, Tabel S (2009) Removal of persistent pollutant chlorobenzene by adsorption onto activated montmorillonite. Appl Clay Sci 43:503–506. https://doi.org/10.1016/j.clay.2008.06.019
17. Mohan A, NimishaK V, Janardana C (2017) Removal of chlorobenzene and 1,4 dichlorobenzene using novel poly-o-toluidine zirconium(IV) phosphotellurite exchanger. Resour Effect Technol 3:317–328. https://doi.org/10.1016/j.reffit.2017.02.003
18. Zulfikar MA, Novita E, Hertadi R, Djajanti SD (2013) Removal of humic acid from peat water using untreated powdered eggshell as low-cost adsorbent. Int J Environ Sci Technol 10:1357–1366. https://doi.org/10.1007/s13762-013-0204-5
19. Ghaedi AM, Vafaei A (2017) Application of artificial neural network for adsorption removal of dyes from aqueous solution: a review. Adv Colloid Interface Sci 245:20–39. https://doi.org/10.1016/j.cis.2017.04.015
20. Khan T, Mustafa MRU, Isa MH, Abd Manan TSB, Ho YC, Lim JW, Yusof NZ (2017) Artificial neural network (ANN) for modelling adsorption of lead (Pb(II)) from aqueous solution. Water Air Soil Pollut 228:426. https://doi.org/10.1007/s11270-017-3613-0
21. Kooh MRR, Dahri MK, Lim LBL (2018) Jackfruit seed as low-coast adsorbent for removal of malachite green: artificial neural network and random forest approaches. Environ Earth Sci 77:432. https://doi.org/10.1007/s12665-018-7618-9
22. Hafsa N, Rushd S, Al-Yaari M, Rahman M (2020) A generalized method for modeling the adsorption of heavy metals with machine learning algorithms. Water 12(12):3490. https://doi.org/10.3390/w12123490
23. Ghaedi M, Ghaedi MM, Negintaji E, Ansari A, Vafaei A, Rajabi M (2014) Random forest model for removal of bromophenol blue using activated carbon obtained from *Astragalus bisulcatus* tree. J Ind Eng Chem 25:1793–1803. https://doi.org/10.1016/j.jiec.2013.08.033
24. Aghajani K, Tayebi H (2017) Adaptive Neuro-Fuzzy Inference system analysis on adsorption studies of Reactive Red 198 from aqueous solution by SBA-15/CTAB composite. Spectrochim Acta A 171:439–448. https://doi.org/10.1016/j.saa.2016.08.025
25. Trifi A, Bouallegue MC, Trifi IM (2019) Application of response surface methodology for optimization of methyl red adsorption by orange peels. Desalin Water Treat 154:369–375. https://doi.org/10.5004/DWT.2019.24086
26. Saores ARDMR, Carvalho FDO, Silva CEDF, Gonçalves AHDS (2020) Random forest as promising application to predict basic-dye biosorption process using orange waste. J Environ Chem Eng 8:103952. https://doi.org/10.1016/j.jece.2020.103952
27. Delvnavaz M (2015) Application of artificial neural networks for prediction of photocatalytic reactor. Water Environ Res 87:113–122. https://doi.org/10.2175/werd1400430.1
28. Mahmoudi NM, Taghizadeh M, Taghizadeh A (2018) Mesoporous carbons of low coast agricultural bio-wastes with high adsorption capacity: preparation and artificial neural network modelling dye removal from single and multicomponent (binary and ternary) systems. J Mol Liq 298:217–228. https://doi.org/10.1016/j.molliq.2018.07.108
29. Khanchoul K, Mahmoud T, Bissonnais YL (2014) Assessment of the artificial neural networks to geomorphic modelling of sediment yield for ungauged catchments, Algeria. J Urban Environ Eng 8:175–185. https://doi.org/10.4090/juee.2014.v8n2.175185
30. Breiman L (2001) Random forests. Mach Learn 45:5–32. https://doi.org/10.1023/A:1010933404324
31. Iskenderoglu FC, Baltacioglu MK, Demir MH, Baldinelli A, Bidini G (2020) Comparison of support vector regression and random forest algorithms for estimating the SOFC output voltage by considering hydrogen flowrate. Int J Hydrogen Energy 45:35023–35038. https://doi.org/10.1016/j.ijhydene.2020.07.265
32. Melcher M, Schoul T, Spangel B, Luchner M, Csejan M, Bayer K, Leish F, Striedner G (2015) The potential of random forest and neural network for biomass and recombinant protein modelling in

Escherichia coli fed-batch fermentation. Biotechnol J 10:1770–1782. https://doi.org/10.1002/biot.201400790
33. Chagas CDS, Junior WDC, Bhering SB, Filho BC (2016) Spatial prediction of soil surface texture in semiarid region using random forest and multiple linear regressions. CATENA 139:232–240. https://doi.org/10.1016/j.catena.2016.01.001
34. Zhang H, Wu P, Yin A, Yang X, Zhang M, Gao C (2017) Prediction of soil organic carbon in an intensively managed reclamation zone of eastern China: a comparison of multiple linear regressions and the random forest. Sci total Environ 15:704–713. https://doi.org/10.1016/j.scitotenv.2017.02.146
35. Kooh MRR, Dahri MK, Lim LB, Lim LH, Lee SL (2019) Phytoextraction capability of *Azolla pinnata* in the removal of rhodamine B from aqueous solution: artificial neural network and random forests approaches. Appl Water Res 80:1–9. https://doi.org/10.1007/s13201-019-0960-6
36. Shrivastava R, Mahalingarm H, Dutta NN (2017) Application and evaluation of random forest classifier technique for default detection in bioreactor operation. Chem Eng Commun 204:591–598. https://doi.org/10.1080/00986445.2017.1292259
37. Boudiaf HZ, Boutahala M, Sahnoun S, Tiar C, Goumri F (2014) Adsorption characteristics, isotherm, kinetics, and diffusion of modified natural bentonite for removing the 2,4,5-trichlorophenol. Appl Clay Sci 90:81–87. https://doi.org/10.1016/j.clay.2013.12.030
38. Aliouane N, Hammouche A, De Doncker RW, Telli L, Boutahala M, Brahimi B (2002) Investigation of hydrations and protonic conductivity of H-montmorillonite. Solid State Ion 148:103–110. https://doi.org/10.1016/S0167-2738(02)00049-8
39. Dammak N, Fakhfakh N, Fourmentin S, Benzina M (2015) Treatment of gas containing hydrophobic VOCs by adsorption process on raw and intercalated clays. Res Chem Intermed 41:5475–5493. https://doi.org/10.1007/s11164-014-1675-9
40. Erdem B, Özcan AS, Özcan A (2010) Preparation of HDTMA-bentonite: characterization studies and its adsorption behaviour toward dibenzofuran. Surf Interface Anal 42:1351–1356. https://doi.org/10.1002/sia.3230
41. Bousba S, Bougdah N, Messikh N, Magri P (2018) Adsorption removal of humic acid from water using a modified Algerian bentonite. Phys Chem Res 6:613–625. https://doi.org/10.22036/pcr.2018.129154.1482
42. Gandhidasan P, Mohandes MA (2008) Prediction of vapor pressure of aqueous desiccants for cooling applications by artificial neural network. Appl Therm Eng 28:126–135. https://doi.org/10.1016/j.applthermaleng.2007.03.034
43. Zhao L, Dai T, Qiao Z, Sun P, Hao J, Yang Y (2020) Application of artificial intelligence to wastewater treatment: a bibliometric analysis and systematic review of technology, economy, management, and wastewater reuse. Process Saf Environ Prot 133:169–182. https://doi.org/10.1016/j.psep.2019.11.014
44. Messikh N, Bougdah N, Bousba S (2017) The use of the multilayer perceptron (MLP) for modelling the phenol removal by emulsion liquid membrane. J Environ Chem Eng. https://doi.org/10.1016/j.jece.2017.06.053
45. Igwegbe CA, Mohmmadi L, Ahmadi S, Rahdar A, Khadkhodaiy D, Dehghani R, Rahdar S (2019) Modelling of adsorption of methylene blue dye on Ho-$CaWO_4$ nanoparticles using Response Surface Methodology (RSM) and Artificial Neural Network (ANN) techniques. MethodsX 6:1779–1797. https://doi.org/10.1016/j.mex.2019.07.016
46. Vaferi B, Bahmani M, Keshavarez P, Mawla D (2014) Experimental and theoretical analysis of the UV/H_2O_2 advanced oxidation processes treating aromatic hydrocarbons and MTBE from contaminated synthetic wastewater. J Environ Chem Eng 2:1252–1260. https://doi.org/10.1016/j.jece.2014.05.016
47. Kolay E, Baser T (2014) Estimation of the dry unit weight of compared soils using general linear model and multi-layer perceptron. Appl Soft Comput 18:223–231. https://doi.org/10.1016/j.asoc.2014.01.033
48. Fridman JH, Heulman JJ (2003) Multiple additive regression trees with application in epidemiology. Stat Med 22:1365–1381. https://doi.org/10.1002/sim.1501
49. Guo PT, Li MF, Luo W, Tang QF, Liu ZW, Li ZM (2015) Digital mapping of soil organic matter for rubber plantation at regional scale: an application of random forest plus residual kriging approach. Geoderma 238:49–59. https://doi.org/10.1016/j.geoderma.2014.08.009
50. Were K, Bui DT, Dick OB, Singh BR (2015) A comparative assessment of support vector regression, artificial neural networks, and random forest for predicting and mapping soil organic carbon

stock across an Afromontane landscape. Ecol Ind 52:394–403. https://doi.org/10.1016/j.ecolind.2014.12.028
51. Meroufel B, Benali O, Benyahia M, Benmoussa Y, Zenasni M (2013) Adsorptive removal of anionic dye from aqueous solutions by Algerian kaolin: characteristics, isotherm, kinetic and thermodynamic studies. J Mater Environ Sci 4:482–491
52. Igwegbe CA, Onyechi PC, Onukwuli OD, Nwokedi IC (2016) Adsorptive treatment of textile wastewater using activated carbon produced from *Mucuna pruriens* seed shells. World J Eng Technol 4:21–37. https://doi.org/10.4236/wjet.2016.41003
53. Kim D, Ryoo KS (2015) A study on adsorption of Li from aqueous solution using various adsorbents. Bull Korean Chem Soc 36:1089–1095. https://doi.org/10.1002/bkcs.10200
54. Dada A, Olalekan A, Olatunya A, Dada O (2012) Langmuir, Freundlich, Temkin and Dubinin–Radushkevich isotherms studies of equilibrium sorption of Zn^{2+} unto phosphoric acid modified rice husk. IOSR J Appl Chem 3:38–45. https://doi.org/10.9790/5736-0313845
55. Luna JL, Montes LER, Vargas SM, Martínez AI, Ricardez OFM, Chavez MCAG, Gonzalez RC, Domingues FAS, Diaz MCC, Hipólito VV (2019) Linear and nonlinear kinetic and isotherm adsorption models for arsenic removal by manganese ferrite nanoparticles. SN Appl Sci 1(8):1–19. https://doi.org/10.1007/s42452-019-0977-3
56. Bilal M, Ali AZ, Soomro U, Muqeet M, Ahmed Z (2020) Adsorption of Indigo Carmine dye onto the surface-modified adsorbent prepared from municipal waste and simulation using deep neural network. J Hazard Mater 408:124433. https://doi.org/10.1016/j.jhazmat.2020.124433
57. Palmer DS, O'Boyle NM, Glen RC, Mitchell JBO (2007) Random forest models to predict aqueous solubility. J Chem Inf Model 47:150–158. https://doi.org/10.1021/ci060164k
58. Makariou D, Barrieu P, Chen Y (2021) A random forest based approach for predicting spreads in the primary catastrophe bond market. Insur Math Econom. https://doi.org/10.1016/j.insmatheco.2021.07.003
59. Ashraf M, Bagherian G, Chamjangali MA, Goudarzi N (2016) Application of linear and non-linear methods for modeling removal efficiency of textile dyes from aqueous solutions using magnetic Fe_3O_4 impregnated onto walnut shell. Spectrochim Acta A 265:120292. https://doi.org/10.1016/j.saa.2016.07.049
60. Ashraf M, Bagherian G, Chamjangali MA, Goudarzi N (2018) Application of artificial neural network and random forest methods for modeling simultaneous adsorption of safranin-O and methyl violet dyes onto modified pine cone powder. Desalin Water Treat 109:90–103. https://doi.org/10.5004/DWT.2018.21920
61. Saha PD, Srivastava J, Chowdhury S (2003) Removal of phenol from aqueous solution by adsorption onto seashells: equilibrium, kinetic and thermodynamic studies. J Water Reuse Desalin 3:119–127. https://doi.org/10.2166/wrd.2013.070
62. Wang YQ, Zhang Z, Li Q, Liu YH (2012) Adsorption of uranium from aqueous solution using HDTMA-pillared bentonite: isotherm, kinetic and thermodynamic aspects. J Radioanal Nucl Chem 293:231–239. https://doi.org/10.1007/s10967-012-1659-4
63. Garson GD (1991) Interpreting neural networks connection weights. AI Expert 6(7):47–51
64. Chen C, Chen Z, Shen J, Kang J, Zhao S, Wang B, Chen Q, Li X (2021) Dynamic adsorption models and artificial neural network prediction of mercury adsorption by a dendrimer-grafted polyacrylonitrile fiber in fixed-bed column. J Clean Prod 310:127511. https://doi.org/10.1016/j.jclepro.2021.127511
65. Bougdah N, Messikh N, Bousba S, Djazi F, Magri P, Rogalski M (2021) Adsorption of toluene from aqueous solutions onto polyethylene glycol modified bentonite: kinetic, isotherm studies and artificial neural network modeling. Desalin Water Treat 231:131–142. https://doi.org/10.5004/dwt.2021.27490
66. Çelekli A, Birecikligil SS, Geyik F, Bozkurt H (2012) Prediction of removal efficiency of Lanaset Red G on walnut husk using artificial neural network model. Bioresour Technol 103(1):64–70. https://doi.org/10.1016/j.biortech.2011.09.106

Authors and Affiliations

Nabil Bougdah[1,3] · Salim Bousba[2,4] · Youghourta Belhocine[1] · Nabil Messikh[1]

[1] Département de Génie des procédés, Faculté de Technolgie, Université 20-Aout-1955, Skikda, Algeria

[2] Département de Génie des procédés, Faculté de Génie des procédés, Université Salah Boubnider Constantine 3, Constantine, Algeria

[3] Laboratoire LRPCSI, Université 20-Aout-1955, Skikda, Algeria

[4] Laboratoire de recherche sur le Médicament et le Développement Durable « ReMeDD », Université Salah Boubnider Constantine 3, Constantine, Algeria